JJMIE

Volume 15, Number 5, December. 2021
ISSN 1995-6665
Pages 461 – 474

Jordan Journal of Mechanical and Industrial Engineering

On the Use of Rigid-Body-Translations for Determining Surface Tilt Angles in Two-dimensional Digital Image Correlation Experiments: A Generalized Approach

Ala Hijazi

Department of Mechanical Engineering, German Jordanian University, Amman, Jordan

Received July 26 2021 *Accepted October 20 2021*

Abstract

The two-dimensional digital image correlation (2D-DIC) technique is used for making full-field in-plane deformation/strain measurements on planar surfaces. One of the basic requirements for making measurements using 2D-DIC is to observe the target surface perpendicularly by the camera. Ensuring camera perpendicularity before starting to make measurements using 2D-DIC is important because errors will be induced in the measured displacements/strains if the camera is not oriented properly. During the initial setting of an experimental setup, small camera misalignment angles of one or two degrees can easily go undetected. This paper reports a simple and reliable approach for verifying the camera perpendicularity in 2D-DIC experiments, and for measuring the tilt angle(s) if the camera is not perpendicular to the surface. The approach uses in-plane rigid-body-translation where the strain error(s) obtained from DIC measurements are used to calculate the tilt angle(s). The translation can be either parallel to the target plane (done by moving the target) or parallel to the camera plane (done by moving the camera) where a different set of equations is used for calculating the tilt angles in each scenario. A translation of a known magnitude in any in-plane direction (parallel to the *x* or *y* axes of the image, or at any angle in between) is all what is required to calculate the tilt angle(s). The approach is also capable to determine the tilt angles if the target is tilted about any of the two in-plane axes (*x* or *y*) or about the two axes simultaneously. Several rigid-body-translation experiments are performed under different conditions to evaluate the validity and accuracy of this approach at tilt angles between 1° and 4°. The results show that tilt angles as small as 1° can be calculated accurately, and that rigid-body-translation as small as 2% of the field-of-view width can be used for making measurements with good accuracy.

© 2021 Jordan Journal of Mechanical and Industrial Engineering. All rights reserved

Keywords: Digital image correlation; 2D-DIC; normal strain error; shear strain error; strain bias; camera non-perpendicularity; camera misalignment; tilt angle; rigid-body-translation.

1. Introduction

Digital image correlation (DIC) is a non-contact technique that provides full-field measurements of surface movements (both deformation and rigid-body motion) using digital images. Such measurements are performed by monitoring the relative movements of unique features on the surface of a body or a structure under load. Since most surfaces do not have unique features for cameras to trace, random speckle patterns are usually painted on the surface. The DIC technique was first introduces in the early 1980s, and over the years, it underwent continuous improvements [1]. With the improved resolution and performance of digital cameras, the DIC technique has rapidly evolved, and it has found its way in more and more applications. Today, DIC has been successfully utilized in a very wide variety of applications ranging from mechanical, aerospace, structural, civil, electronics, materials, and manufacturing engineering, to non-destructive testing and evaluation, to biomedical and life sciences [1-16]. Also, DIC can be performed using images ranging in scale from microscopic (even scanning electron microscopy) images all the way up to images of full-scale structures, and ranging in capture speed from few frames per second (fps) all the way to more than one million fps [1-6, 17-20]. Furthermore, DIC has also found use in high temperature applications using images captured in the ultraviolet spectrum [21]. Besides the good measurement accuracy of the DIC technique, it also offers some of attractive features such as; relatively low cost equipment, relatively simple experimental setup, simple or no specimen preparation and not so strict requirements for the measurement environment. Due to its capabilities and advantages, DIC has now become the most widely used technique for non-contact full-field surface motion and deformation measurements.

The DIC technique has two variations; 2D-DIC and 3D-DIC. The 2D-DIC is the simplest version of the technique where images are recorded using one camera, and these images are used for making in-plane motion and deformation measurements of planar surfaces. On the other hand, the 3D-DIC uses two (or more) cameras in stereo configuration that capture simultaneous image sequences, and it is capable of making three-dimensional measurements on surfaces of any shape. Both the 2D-DIC and 3D-DIC are increasingly being used in a wide variety

* Corresponding author e-mail: Ala.Hijazi@gju.edu.jo.

of research and industrial applications [1-6]. In general, the 3D-DIC is more robust, and it offers more capabilities than 2D-DIC.But nevertheless, the 2D-DIC offers some advantages that make it more appropriate for use in some situations, and in general, it is more suitable for testing done in the field. The advantages of 2D-DICare; lower initial cost for both the equipment and software, lower computational cost, ease of use, and the relatively less stringent requirements for the experimental setup (e.g., calibration is generally not required). Practically, three conditions/assumptions need to be satisfied in order to make accurate deformations/strains measurements using 2D-DIC. These conditions are: i) the specimen should have a planar surface, ii) the specimen should undergo pure in-plane motion/deformation (i.e., no out-of-plane component of the motion), and iii) the camera should be oriented perpendicularly relative to the surface of the specimen. In addition, there are several other factors, or sources of error, that can affect the accuracy of 2D-DIC measurements, and there are numerous research studies addressing the error assessment in 2D-DIC and DIC in general [1, 22-26]. These factors include: I) the speckle pattern (density, contrast, size distribution, etc.), ii) the imaging system (lens optical distortions, sensor type, noise, resolution, camera and lens settings etc.), and iii) the selection of the correlation algorithm and parameters (subset and step sizes, correlation and shape functions, sub-pixel interpolation algorithm, etc.). One of the simplest and most widely accepted approaches for assessing the level of baseline error in DIC measurements is the use of rigid-body-translation experiments, which was first introduced by Chu et al. [27]. For 2D-DIC, when the target surface undergoes an in-plane rigid-body-translation, the strains measured by the DIC software should theoretically be zero. Therefore, any strains obtained by DIC during such translation, simply reflects an error in the strain measurements. In experiments where 2D-DIC is to be used, before running the actual experiments, it is usually recommended to perform an in-plane rigid-body-translation experiment (under the same settings and conditions to be used in the actual experiments) in order to estimate the overall level of strain error (both the bias and random error) in the DIC measurements.

For 2D-DIC measurements, as stated earlier, the specimen is assumed to undergo in-plane motion/deformation only (i.e., no out-of-plane motion) and to be perpendicular to the camera viewing axis. The satisfaction these two conditions are essential to the accuracy of the measurements. In general, out-of-plane translations and/or rotations may occur during the loading of the specimen, and several studies have investigated errors associated with such cases. Haddadi et al. [23] estimated the strain errors resulting from out-of-plane translations using rigid-body-translation experiments. Sutton et al. [28] studied the effects of out-of-plane translations/rotations both theoretically and experimentally and showed that such error can be significant, and that it is inversely proportional to the distance between the camera and the surface. Siddiqui [29] proposed a method for eliminating the displacement bias caused by out-of-plane motion through including the possible modes of global rigid-body motion of the specimen surface within the calculation of in-plane displacements. Pan et al. [30] used rigid-body-translation experiments to study the strain error resulting from out-of-plane translations, and they proposed a method to compensate for the effect of out-of-plane translation using a non-deformable reference sample. Badaloni et al. [31] examined the error caused by out-of-plane movement during cyclic loading and proposed a method to compensate for such error using non-deformable plates fixed on the surface of the specimen. Halding et al. [32] proposed a method for the correction of strain measurements for the effect of out-of-plane motion (including rotation) of the surface. They applied their method for measuring strains in bridges using wide-angle lens camera during load testing.

Besides the out-of-plane translation and/or rotation that might occur during the experiments, it is also possible to have an inappropriate alignment of the camera such that it is not observing the surface perpendicularly. Such camera non-perpendicularity can exist before loading starts, and it remains throughout the experiment. Some researchers have investigated the measurement errors associated with the cases where the camera axis is not perpendicular to the target surface. Meng et al. [33] studied the effect of the non-perpendicular camera alignment on the measurement accuracy of in-plane displacements. Based on theoretical analysis, they reported that measurement sensitivity of 0.01 pixels could be attained under misalignment angles up to 5° (for the parameters used in their investigation). Lava et al. [34] studied the strain errors induced by non-perpendicular camera alignment using numerically tilted images having an imposed finite element displacement field. They proposed an image rectification method for eliminating the image distortion caused camera non-perpendicularity (such that the images will be suitable for 2D-DIC), and they compared the strain error for a sample subjected to large plastic strain using 2D-DIC and 3D-DIC. Such image rectification approach can be useful when there are physical/experimental constrains that prevent the camera from being oriented perpendicularly, given that the surface tilt angle is known. Wang et al. [35] proposed a method of compensation for both out-of-plane motion (including out-of-plane translation and out-of-plane rotation) and non-perpendicular alignment, in order to improve the accuracy of 2D-DIC measurements. Their method is based on projecting a cross-shaped structured light pattern on the surface of the specimen and using triangulation to calculate the out-of-plane translation/rotation from the deformation of the structured light. The obtained out-of-plane motion information is then used to compensate the strains measured by DIC. They conducted experiments with controlled out-of-the-plane motions to verify their proposed approach and reported that the mean error after compensation can be as small as 50 μ-strains. Hijazi et al. [36] investigated the errors in strain measurements caused by non-perpendicular camera alignment both theoretically and experimentally. They developed analytical equations for determining the magnitude of the strain error (bias) resulting from camera non-perpendicularity. They showed that camera non-perpendicularity cause errors to be induced in both the normal and shear strains, and that a strain error greater than 10^3 μ-strains can result from misalignment angles as small as 2°. In general, a translation perpendicular to the tilt axis causes apparent normal strains while a translation parallel to the tilt axis causes apparent shear strain. These non-zero strains (i.e., strain errors) can be observed when performing DIC on images of tilted specimens undergoing in-plane rigid-body-translations. Furthermore, a non-perpendicular alignment will cause bias in the strain readings when performing DIC on images of a specimen undergoing actual deformation. In-plane rigid-body-translation experiments were used to validate the analytical equations, and the results were found to be in a very close agreement. Later, Hijazi [37] introduced a novel approach for verifying camera perpendicularity and calculating the camera tilt angle (if the camera is not perpendicular to the target surface). This approach is intended to be used as a verification/calibration step during the initial setting of 2D-DIC experiments (i.e., before starting to use the experimental setup for actual measurements). The approach is based on the strain error equations developed previously by Hijazi et al. [36]. These equations were simplified and solved to obtain the tilt angle(s) of the target surface based on the strain error(s) caused by camera non-perpendicularity. The essence of the approach is to do a simple in-plane rigid-body-translation experiment, then to use the developed equation(s) to calculate the tilt angle(s) base on the strain error(s) obtained from DIC analysis. The approach involves doing the rigid-body-translation using the same specimen to be tested (before running the actual experiment) where the translation can be in either of the two in-plane directions (*x* or *y*). The approach was validated experimentally and it was shown that it has accuracy better than 0.3°, and that it can be used to measure tilt angles as small as 1° about any of the two in-plane axes.

During the initial setting of an experimental setup where 2D-DIC is being used, care is usually taken to align the camera perpendicular to the target surface. The camera alignment is usually done using mounting hardware and simple measuring tools (translating stages, right angle triangles, tape measures, inclinometers, etc.). When the distance between the camera and the target is relatively small, ensuring camera perpendicularity can be somewhat easy. However, as the working distance between the camera and target becomes larger, ensuring camera perpendicularity becomes more difficult, and small camera misalignment angles of one or two degrees can easily go undetected. Up to the knowledge of the author, there are no methods for ensuring camera perpendicularity in such cases reported in literature. The novel method for determining the tilt angles proposed by Hijazi [37] was the first and still the only method reported in literature for ensuring camera perpendicularity and estimating the tilt angles in 2D-DIC experiments (where only one camera is used). In this paper, a more generalized approach for determining the surface tilt angle(s) using rigid-body-translation experiments is presented. The approach initially proposed by Hijazi [37] is extended in this paper to address some cases that were not considered previously, and some of the practical issues related to the use of this approach are also addressed. The case where the translation is parallel to the plane of the camera (rather than the target) is investigated here and new equations for the strain error and for calculating the tilt angle are developed for this case. The translation parallel to the camera can be done by moving the camera itself, and such approach can be useful when it is not possible to do the rigid-body-translation using the target. Additionally, while the work presented in Hijazi [37] only considers translations that are either parallel or perpendicular to the tilt axis, the case where the translation is in some arbitrary in-plane direction (i.e., it has both *x* and *y* components) is considered here. Furthermore, the case where the target is tilted about both the *x* and *y* axes, simultaneously, is also investigated. Moreover, in some practical cases, it might not be possible to do large translations. Thus, the feasibility of using very small translations (as small as 1% of the field-of-view width) for performing measurements is investigated. Finally, the effect of the distance between the camera and the target on the measurement accuracy is demonstrated. All the above-mentioned cases are investigated experimentally, and the results of these validation experiments are presented in this paper.

2. Theory

Perpendicularity of the camera's optical axis with respect to the surface being observed is one of the conditions for the validity of 2D-DIC measurements. If there is a misalignment between the camera plane and the target surface, in-plane translations of the surface will not be accurately depicted at the camera's imaging sensor. Accordingly, when DIC analysis is performed using such images, even if the surface is undergoing a pure in-plane rigid-body-translation, it will appear as if it is being deformed (i.e., there will be nonzero strains). Previous investigations have shown that non-perpendicular camera alignment causes strain errors (in the form of bias) where the type and magnitude of these strain errors depend on the direction of the in-plane translation relative to the tilt axis of the camera (or target) [36, 37]. When the target surface translates perpendicular to the tilt axis, normal strain error will be induced. On the other hand, when the surface translates parallel to the tilt axis, shear strain error will be induced. Based on the pinhole camera model along with the small-strains theory (Cauchy strain), Hijazi et al. [36] developed theoretical equations for determining the normal and shear strain errors resulting from camera non-perpendicularity. These equations show that the strain errors are proportional to the misalignment (or tilt) angle, and they are also function of the direction and magnitude of the rigid-body-translation, as well as the stand-off-distance between the camera and the surface. Later, Hijazi [37] further developed these strain error equations and introduced a novel approach for calculating the surface tilt angle(s) based on the apparent DIC strain(s) error. This approach utilizes simple in-plane rigid-body-translation (in the direction parallel or perpendicular to the tilt axis) to measure the normal and shear strain errors caused by camera non-perpendicularity using DIC analysis. It then calculates the tilt angle(s) using simple analytical equations based on the measured strain error. This simple approach is meant to be used as a verification/calibration step during the initial setup of 2D-DIC experiments (i.e., before starting to use the setup for actual measurements). By translating the target in any of the two in-plane directions (horizontal or vertical), the tilt angles about the axis parallel and the axis perpendicular to the direction of translation (if any exists) can be calculated. Three simple equations were developed for calculating the surface tilt angle, which are [37]:

$$\theta_{\perp} \cong \sin^{-1}\left[\frac{\varepsilon_{xx}S}{2\Delta x + \varepsilon_{xx}(\Delta x - x_A)}\right] \quad (1)$$

$$\theta_{\perp} = \sin^{-1}\left[\frac{\varepsilon_{yy}S}{\Delta x + \varepsilon_{yy}(\Delta x - x_A)}\right] \quad (2)$$

$$\theta_{/\!/} = \tan^{-1}\left(\frac{2\varepsilon_{xy}S}{\Delta y}\right) \quad (3)$$

where ε_{xx}, ε_{yy} and ε_{xy} are the strain errors resulting from rigid-body-translation (obtained from DIC analysis), S is the target stand-off-distance, x_A is the x coordinate of a point on the surface (usually $x_A = 0$ is used), Δx & Δy are the magnitudes of rigid-body-translation in the x and y directions. In fact, all the three equations theoretically give the same tilt angle. The first two equations are used (any one of them can be used) to find the tilt angle (denoted as $\theta_{\perp}$) based on the DIC normal strain errors (ε_{xx} or ε_{yy}) resulting from rigid-body-translation perpendicular to the tilt axis. The third equation, on the other hand, is used to find the tilt angle (denoted as $\theta_{/\!/}$) based on the DIC shear strain (ε_{xy}) error resulting from rigid-body-translation parallel to the tilt axis. It is probably worth mentioning here that equation 1 is based on an approximate solution for the normal strain (ε_{xx}) error, yet it was shown to be fairly accurate [37]. It is also important to note that this approach is capable of determining not only the magnitude of the tilt angle, but also the direction of rotation (or sense). The direction of rotation can be determined based on the sign of the strain error where the tilt angle will have the same sign as the strain error obtained from the DIC analysis. For non-perpendicular camera orientation, the sign of the strain error in DIC analysis depends on the direction of translation (flipping the reference and deformed images in DIC analysis will flip the sign). Hence, the direction of rotation can be identified relative to the direction of translation. In addition, it should be noted here that, though DIC software packages use the large strains theory (Green-Lagrange strain) for calculating strains, small strains theory was used for deriving the theoretical strain error equations where that is justified based on the fact that the strains resulting from camera non-perpendicularity are relatively small (given that the tilt angles are small). The resulting strain error obtained by these equations was also validated experimentally by comparing with DIC results [36].

The equations developed previously by Hijazi [37] (equations 1 to 3) assume that the rigid-body-translation is parallel to the plane of the target. To further generalize the approach, in the work presented herein, the case where the rigid-body-translation is parallel to the camera plane (rather than the target plane) is also considered. To illustrate the difference between the two cases, Figure 1 shows a schematic representation of a non-perpendicular camera setup. In the figure, the coordinate system is defined relative to the target surface where the z axis is normal to the surface and the target is tilted by angle θ about the y axis (x and y are the in-plane axes of the target). If the surface is not tilted (i.e., camera perpendicular to the target surface) the axes of the coordinate systems of the camera and the target will be all parallel. The figure also illustrates that the translation of the target along the x direction (i.e., the direction perpendicular to the tilt axis) can be either parallel to the target plane (Δx) or parallel to the camera plane (Δx_c). The strain errors resulting from translations parallel to the target plane and how they can be used to determine the surface tilt angle were illustrated in a previous investigation [37]. The effect of translations parallel to the camera plane and how to use the resulting DIC strain error(s) to determine the tilt angle are presented in this investigation. It should be stressed here that in actual DIC experiments, a translation parallel to the camera plane would most likely be performed by translating the camera itself. However, theoretically it does not make a difference whether the camera or the target are translated as long as the translation is parallel to the camera plane.

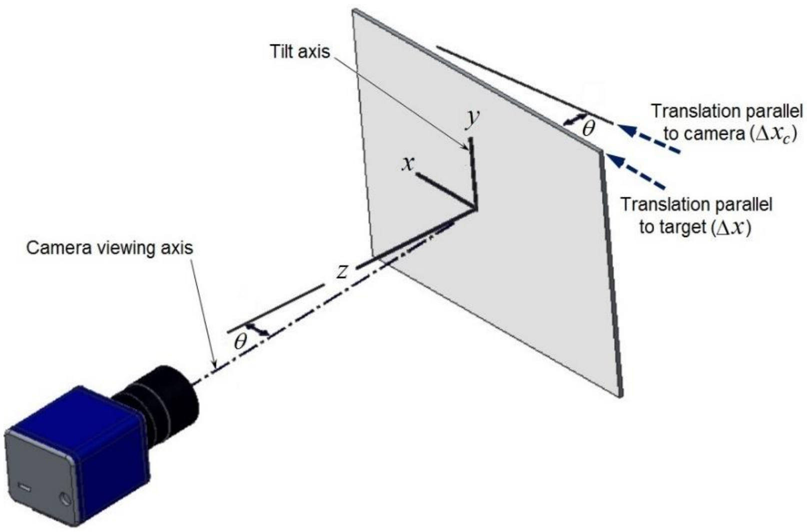

Figure 1. Schematic illustration of the orientation of a non-perpendicular camera setup.

A schematic illustration of the pinhole camera model and how it resembles a real camera is shown in figure 2. In the figure, the image plane identifies the location of the camera's imaging sensor or focal plane array (FPA) while the location of the pinhole plane represents the mid-thickness of the lens. The distance f in the figure (i.e., the distance between the pinhole plane and the image plane) represents the focal length of the lens. It might be worth mentioning here that for multi-element lenses typically used in imaging, the physical distance from the lens mid-thickness to the FPA is slightly different from the focal length of the lens; yet still, this geometric model holds true. The distance S between the pinhole plane and the object is referred to as the stand-off-distance. This stand-off-distance is slightly larger than the actual distance from the front end of the lens body to the target surface (usually referred to as the working distance) as will be further discussed later. According to the pinhole model, an object of length $l$will have a projected length of l^i at the image plane (assuming that the object is parallel to the image plane) where:

$$l^i = \frac{l}{S} f \tag{4}$$

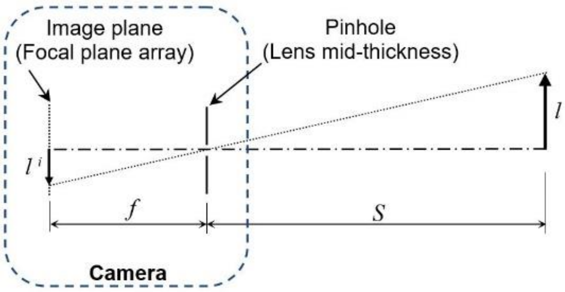

Figure 2. Schematic illustration of the pinhole camera model.

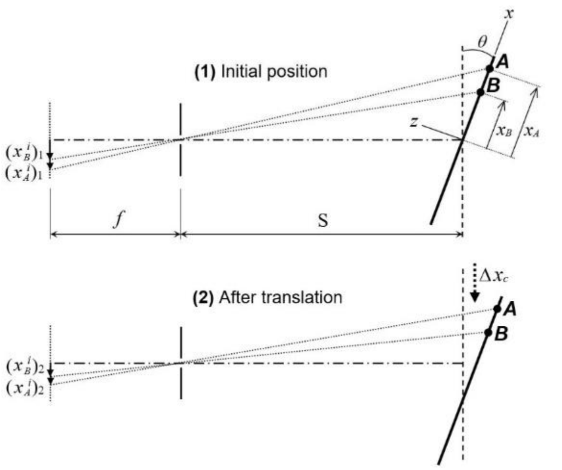

Figure 3. Pinhole camera schematic of a tilted surface translating perpendicular to tilt axis (the translation is parallel to the camera plane).

Figure 3 shows a schematic planar representation of a pinhole camera imaging a target surface tilted by angle θ (about the y axis). This figure actually represents a top projection view of the setup seen in figure 1, and the same notations are used in both figures. The surface is considered to rigidly translate by a distance Δx_c (in the direction parallel to the camera plane). For clarity, the positions of the surface before and after the translation are shown in two separate sketches as seen in the figure. A line segment is defined on the target surface (along the x direction) between points **A** and **W**here the line segment has a length of l_x. When the surface is at position (**1**), the x coordinates "at the image plane" for points **A** and **B** are found as:

$$\left(x_A^i\right)_1 = \frac{x_A \cos\theta}{S + x_A \sin\theta} f \tag{5}$$

$$\left(x_B^i\right)_1 = \frac{x_B \cos\theta}{S + x_B \sin\theta} f = \frac{(x_A - l_x)\cos\theta}{S + (x_A - l_x)\sin\theta} f \tag{6}$$

where x_A & x_B are the coordinates of the two points at position (**1**). Using the coordinates "at the image plane", the projected length of line **AB** "at the image plane "can simply be found as:

$$\begin{aligned}\left(l_{AB}^i\right)_1 &= \left(x_A^i\right)_1 - \left(x_B^i\right)_1 \\ &= \left[\left(\frac{x_A}{S + x_A \sin\theta}\right) - \left(\frac{x_A - l_x}{S + (x_A - l_x)\sin\theta}\right)\right]\cos\theta\, f\end{aligned} \tag{7}$$

When the surface moves to position (**2**) after translating a distance Δx_c, the new x coordinates of the two points "at the image plane" become:

$$\left(x_A^i\right)_2 = \frac{x_A \cos\theta - \Delta x_c}{S + x_A \sin\theta} f \tag{8}$$

$$\left(x_B^i\right)_2 = \frac{x_B \cos\theta - \Delta x_c}{S + x_B \sin\theta} f = \frac{(x_A - l_x)\cos\theta - \Delta x_c}{S + (x_A - l_x)\sin\theta} f \tag{9}$$

and therefore the projected length of line **AB** "at the image plane" becomes:

$$\begin{aligned}\left(l_{AB}^i\right)_2 &= \left(x_A^i\right)_2 - \left(x_B^i\right)_2 \\ &= \left[\left(\frac{x_A \cos\theta - \Delta x_c}{S + x_A \sin\theta}\right) - \left(\frac{(x_A - l_x)\cos\theta - \Delta x_c}{S + (x_A - l_x)\sin\theta}\right)\right] f\end{aligned} \tag{10}$$

The average (Cauchy) normal strain for the line segment in the x direction can be calculated as:

$$\varepsilon_{xx} = \frac{\left(l_{AB}^i\right)_2 - \left(l_{AB}^i\right)_1}{\left(l_{AB}^i\right)_1} \tag{11}$$

Substituting equations (7) and (10) into equation (11) and simplifying the resulting expression, both the focal distance f and the line segment length l_x cancel out, and the strain error equation becomes:

$$\varepsilon_{xx} = \frac{\Delta x_c}{S} \tan\theta \tag{12}$$

Equation (12) can be solved to obtain the surface tilt angle based on the normal strain error ε_{xx} obtained from DIC analysis. As used previously in equations (1) and (2), the calculated tilt angle is denoted as $\theta_\perp$ to indicate that this is a tilt angle that is calculated based on a translation in the direction perpendicular to the tilt axis, and it is found as:

$$\theta_\perp = \tan^{-1}\left[\frac{\varepsilon_{xx} S}{\Delta x_c}\right] \tag{13}$$

Similarly, it is necessary to determine whether the translation Δx_c will also induce an “apparent " normal strain in the y direction. Considering a line of length l_y(oriented along the y direction) that is defined at an arbitrary distance along the x axis (assumes for instance a line oriented in the y direction and located at point **A**). By referring to Figure 3 again, it can be seen that the "horizontal" distance from point **A** to the pinhole plane does not change as a result of the translation Δx_c. Since the horizontal distance remains unchanged after the "vertical" translation (Δx_c), any line segment defined in the y direction will still have the same projected length at "the image plane" after the translation Δx_c. Thus, there will be no apparent normal strain in the y

direction as a result of the translation Δx_c (i.e., $\varepsilon_{yy} = 0$). Also, the inspection of the coordinates of the line segments defined along the x and y directions shows that the orientation of these lines will not be affected due to the translation Δx_c. Therefore, it is also concluded that there will be no apparent shear strain error resulting from camera non-perpendicularity when the translation is perpendicular to the tilt axis (i.e., $\varepsilon_{xy} = 0$). For comparison purposes, and to avoid confusion, the strain errors resulting from translations perpendicular to the tilt axis for both cases, parallel to the target plane and parallel to the camera plane, are summarized in Table 1 (equations for translation parallel to camera plane are obtained from Hijazi [37]). A quick comparison of the magnitude of the strain error in the direction of translation (ε_{xx}) shows that when the translation is parallel to the camera plane, the strain error is approximately half of that when the translation is parallel to the target plane (assuming $x_A = 0$, $\Delta x \ll S$, and small angles: $\sin\theta \cong \tan\theta$).

3. Experiments

3.1. Setup

The camera used in this investigation is a 5.5 megapixel monochrome scientific imaging camera (PCO Edge 5.5). This camera has a scientific-Complementary Metal Oxide Sensor (sCMOS) chip with 2560×2160 pixels resolution, 18.8 mm sensor size, and 16 bit dynamic range. The lens used with the camera is a premium quality 50mm focal length lens (ZEISS Milvus 2/50M). During the experiments, the lens aperture is set at f/8 to ensure that the entire target surface is in good focus even when the target is tilted at the maximum tilt angle. The camera is fixed on a sturdy adjustable multi-axis camera-mount to enable the adjustment of the camera orientation. The camera-mount is fixed on an optical rail such that the camera can be moved to any desired working distance without interrupting the camera alignment. The target plate is mounted on a multi-axis high-precision translating/rotating stage such that the desired translations/rotations can be performed. An overall view of the experimental setup is shown in Figure 4. To ensure that the camera is perfectly perpendicular to the target surface before the experiments are started, the camera is first brought into contact with the target surface and its orientation is adjusted; then, the camera is retracted back to the desired working distance. The multi-axis stage used for mounting the target plate allows the target to be translated in the *x* and *y* directions and to be rotated about the *y* axis. As can be seen in the figure, two translating stages are allocated for the translation along the *x* direction where one of them is mounted on top of the rotating stage while the other is below. With such setup, the translating stage on top is used to translate the target parallel to its plane, while the bottom stage is used to translate the target parallel to the camera plane. A printed random speckle pattern (black dots on white background) is affixed to the surface of the target plate. The speckle pattern is generated using a software called "Speckle Generator" with the following parameters; 0.4 mm dot diameter, 60% density, and 80% variation. The working distance between the camera and the target is set such that the field-of-view observed by the camera is 100mm wide (this makes the scale factor to be about 26 pixels/mm and the average dot size is about 10 pixels).The magnification level being used here (i.e., 100 mm field-of-view width) is achieved when the working distance is about 307 mm. It should be kept in mind that the working distance being reported here (i.e., the distance from the front end of the lens body to the target surface) is smaller than the stand-off-distance used in the equations for calculating the tilt angle, as will be discussed later.

3.2. Procedure

Different groups of experiments are carried out in order to validate the proposed approach and evaluate its accuracy in determining the tilt angles. In all the different scenarios being investigated here, the first set of experiments is always performed while the camera is being perfectly perpendicular to the target surface. This done to evaluate the baseline strain error level associated with the imaging system (camera/lens combination) and the DIC setting/parameters [24]. In each of the different groups of experiments, a reference position image is captured, and then other images are captured after the target is translated to different positions. In general, the translations are done in two directions, the *x* direction (i.e., perpendicular to the tilt axis) and the *y* direction (i.e., parallel to the tilt axis). The translation step size for each of the two directions is set to be 5% of the field-of-view width (i.e., 5 mm at the magnification level being used here).

3.2.1. Translations parallel to camera plane

After performing the initial translation experiments while the camera is perpendicular to the target surface, the same translation experiments are repeated after tilting the target at different angles around the *y*-axis starting from 1° up to 4° in 1° steps. In each group of experiments that corresponds to a certain tilt angle, the translation in the *x* direction is made such that it is parallel to the plane of the camera (not the target) where this is achieved by using the top translating stage (see figure 4). As for the translation in the *y* direction, it is done as usual since the *y*-axis is parallel to both the camera plane and the target plane (since it is the tilt axis). In each of the two directions (*x* and *y*), the target is translated in two steps (5mm each); thus, images are recorded for the target at five different positions; a reference position, two positions with translation in the *x* direction, and two positions with translation in the *y* direction.

3.2.2. Translation in two directions simultaneously

In this group of experiments, instead of translating the target along the *x* or *y* directions, the translation is bi-directional such that the translation direction makes an angle with the *x* and *y* axes. As such, the translation will have both an *x* and *y* components at the same time (i.e., the translation is neither parallel nor perpendicular to the *x* or *y* axis, it has an angle with both). Three different angles (measured from the positive *x* axis) are used for the translation which are: 36.9°, 45° and 53.1°. These angular translations are achieved by performing simultaneous translations in the *x* and *y* directions as follows: Δx= 4 mm & Δy= 3 mm (36.9°), Δx= 3 mm & Δy= 3 mm (45°), and Δx= 3 mm & Δy= 4 mm (53.1°). These bi-directional translation experiments are done using translations parallel to the target while the target surface is tilted at 3°.

Table 1. Strain error induced by translation perpendicular to the tilt axis.

Translation direction	Normal strain error in the direction of translation	Normal strain error in the direction perpendicular to translation	Shear strain error
Translation parallel to target plane	$\varepsilon_{xx} \cong \dfrac{2\Delta x \sin\theta}{S + (x_A - \Delta x)\sin\theta}$	$\varepsilon_{yy} = \dfrac{\Delta x \sin\theta}{S + (x_A - \Delta x)\sin\theta}$	$\varepsilon_{xy} = 0$
Translation paralell to camera plane	$\varepsilon_{xx} = \dfrac{\Delta x_c}{S}\tan\theta$	$\varepsilon_{yy} = 0$	$\varepsilon_{xy} = 0$

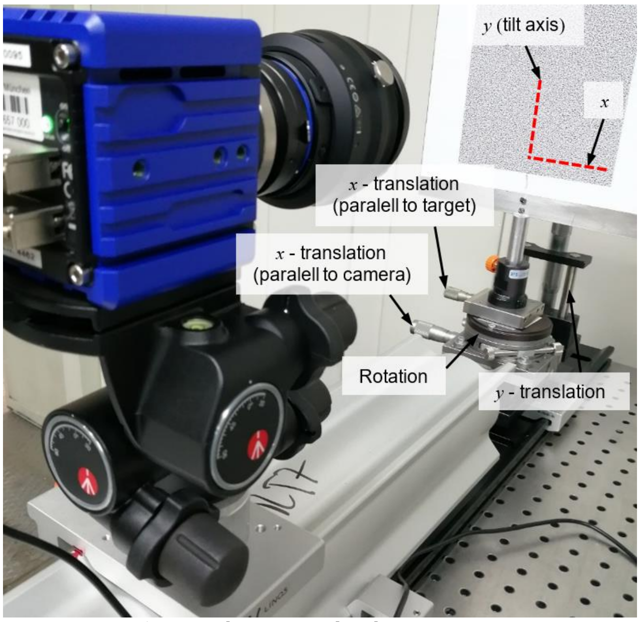

Figure 4. The setup used in the experiments.

3.2.3. Two axes tilting

In this group of experiments, instead of tilting around the vertical axis alone, the target plane is tilted with respect to the camera plane around both the x and *y*-axes. This is done by performing the rotation around the *y* (vertical) axis as usual, while the other rotation is done by tilting the camera about the *x* (horizontal) axis. It should be noted here that performing the rotation about the *x* (horizontal) axis using the camera rather than the target gives basically the same result (it is done this way since the camera is already mounted on a 3-axis rotating stage). The experiment is done at two simultaneous tilt angles of 2° about the y-axis and 1° about the *x* axis. The translations are done (5 mm step as usual) once along the *x* direction and once along they direction.

3.2.4. Small translations

In the previous groups of experiments, the translation step size is set to be 5 mm (i.e., 5% of the field-of-view width); however, a smaller step size is used in this group. Translations are done here starting with a 1 mm step size (1, 2, 3, 5 mm) in the *x* and *y* directions. The experiments are done while the target surface is tilted at 2°.

3.2.5. Different working distance

All the previously mentioned groups of experiments are performed while the working distance is set at 307 mm (from the front end of the lens to the target). To investigate the effect of the working distance on the accuracy of the tilt angles calculated using this approach, two additional groups of experiments are performed at two other values of the working distance. The other two groups of experiments are performed at 197 mm and 417 mm working distance. At 197 mm working distance, the field-of-view width is about 63 mm; while for the 417 mm working distance it is about 137 mm. In order to be comparable with the experiments performed at 307 mm working distance, the steps for the x and y translations are also set to be 5% of the field-of-view width where that gives 3.15 mm and 6.85 mm, for the 197 mm and 417 mm working distances, respectively. The experiments in this group are done while the target surface is tilted at 2°.

3.3. DIC Analysis

For the different groups of rigid-body-translation experiments that are performed here, the reference position image is correlated with the images corresponding to each of the different translated positions. In all experiments, a square region of interest (size of 1600×1600 pixels) located near the center of the image is used in the DIC analysis such that the same number of data points is used in the x and y directions, and thus the same reliability is achieved for the results in both directions. The DIC analysis is performed using the "MatchID-2D" software [38] with the following correlation parameters: normalized cross-correlation algorithm, no image pre-filtering, subset size of 51×51 pixels, step size of 25 pixels, and the "Green-Lagrange" strains are calculated using 7×7 points strain window size.

For the experiments done at different working distance (section 3.2.5), the DIC analysis is performed using different

 © 2021 Jordan Journal of Mechanical and Industrial Engineering. All rights reserved - Volume 15, Number 5 (ISSN 1995-6665)

subset size and step size for each case. For the 197 mm working distance, 81×81 pixels subset size and 40 pixels step size are used; while for the 417 mm working distance, 37×37 pixels subset size and 18 pixels step size are used. This is done to maintain the same physical size for the subset and step sizes, since the same speckle pattern is used in all cases while the images have different magnification levels. It might be worth mentioning here that the speckle dot size at the 417 mm working distance is about 7 pixels which is still large enough to avoid any effect of the camera fill-factor on the accuracy of DIC results [26].

4. Results and Discussion

4.1. Translation Parallel to Camera

The approach developed previously by Hijazi [37] uses rigid-body-translations to verify the perpendicularity of the camera's viewing axis with respect to the target surface; and if the camera is not perpendicular, the resulting strain errors are used to determine the surface tilt angle. In this approach, the direction of translation is considered to be parallel to the plane of the target surface, and the translation can be either parallel or perpendicular to the tilt axis. In fact, performing translations that are parallel to the target surface is feasible in most experimental setups and it can be done by translating the target itself using the same actuator that is used for performing the actual experiments. Nevertheless, in some experimental setups it might be more convenient to do the rigid-body-translation to verify the camera perpendicularity by moving the camera itself rather than the target. In such cases, the camera can be mounted directly on a small one-axis translating stage that allows the camera to move in the horizontal or vertical directions, and the camera can be simply aligned with the translating stage. Consequently, the translation of the camera in this case will be parallel to the camera plane. In this study, it is shown that the strain errors resulting from camera non-perpendicularity are quite different when the translation direction is parallel to the target plane or the camera plane (see Table 1). This difference which is observed from the theoretical strain error equations is further verified experimentally and the results are shown in Figure 5. It is probably worth to mention here that the strain values shown in the figure are the mean values, which are calculated over the entire region of interest used in the DIC analysis. In Figure 5 (a) it can be seen that for a translation perpendicular to the tilt axis and parallel to the target plane, when the camera is not perpendicular to the target, error will be induced in both normal strain components (ε_{xx} and ε_{yy}) while the shear strain (ε_{xy}) is practically not affected. However, as can be seen in Figure 5 (b), when the translation is parallel to the camera plane, error will be induced only in the normal strain component along the direction of translation (ε_{xx}) while the other strain components (ε_{yy} and ε_{xy}) are practically not affected. The theoretical values of the strain error (represented by the solid line) are also shown in the figure for each case, and it can be seen that the experimental results are generally in good agreement with the theoretical values. When the translation is parallel to the target plane, the tilt angle can be calculated based on either ε_{xx} orε_{yy} using equation (1) or (2). It is generally preferable to use equation (1) and calculate the tilt angles based on theε_{xx} error since the ε_{xx} value is larger, thus it is expected to yield results that are more accurate. On the other hand, when the translation is parallel to the camera plane, error will only be induced in ε_{xx} and the tilt angle can be calculated using equation (13). It is important here to notice the big difference in the resulting ε_{xx} error between the two cases where ε_{xx} for the translation parallel to the camera is basically equal to half of that when the translation is parallel to the target. As a matter of fact, this observation calls for caution when using the proposed approach to determine the tilt angles where the experimental setup has to be carefully set to produce translations that are either parallel to the target plane or the camera plane. If the experimental setup is not set correctly and the translation is neither parallel to the target nor the camera, then both equations (1) and (13) will give incorrect tilt angle values. However, it is worth mentioning that even though the equations cannot give the correct value of the tilt angle, the proposed approach can still be used to check whither the camera is perpendicular to the target surface or not by comparing the values of the mean strain error $((1/N)\sum\varepsilon)$ and the mean of the absolute values of strain $((1/N)\sum|\varepsilon|)$. When these two strain error measures have similar magnitudes, this indicates that the camera is not perpendicular to the target surface [36].

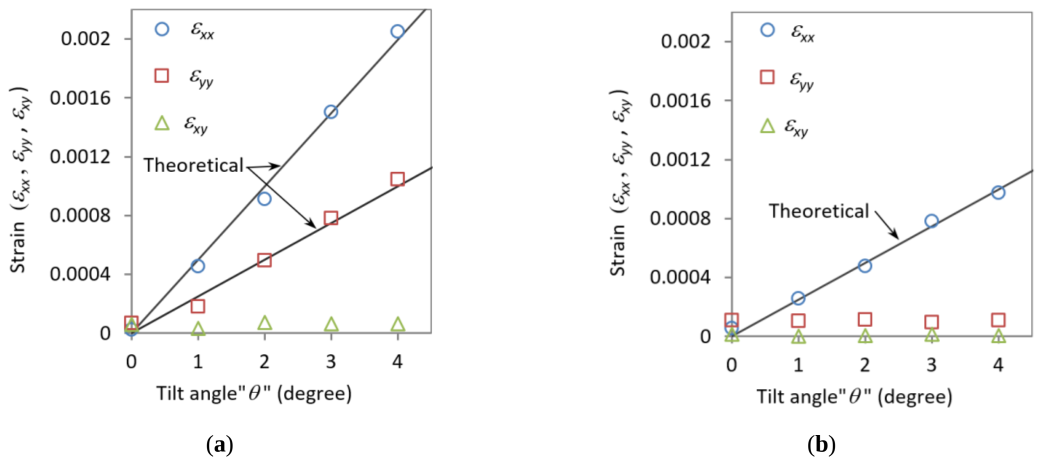

Figure 5. Comparison of the effect of translation direction on strain error (for translations perpendicular to tilt axis): (**a**) Translation parallel to target (Δx = 5 mm), (**b**) Translation parallel to camera (Δx_c = 5 mm).

A graphical comparison of the tilt angles calculated based on translation parallel to the camera plane (using equation 13) with the actual tilt angles is shown in Figure 6. The dashed 45° line shown in the figure represents the equality of the calculated and the actual tilt angle values. In this type of figure, a point above the dashed 45° line indicates that the calculated value is larger than the actual value, while a point below the dashed 45° line indicates that the calculated value is smaller than the actual value. The figure shows the predicted tilt angle values obtained using 5 mm and 10 mm translations, and it can be seen that the calculated tilt angle values are generally in good agreement with the actual tilt angle values. By closely inspecting the results shown in the figure, it can be observed that there is no advantage in terms of accuracy when using larger translation (10 mm). On the contrary, the calculated tilt angle values obtained using 5 mm translation seems to be slightly more accurate. In fact, this observation is actually in agreement with the results presented previously by Hijazi [37], and this is most likely to be attributed to the use of small strains theory in developing the theoretical strain error equations, while the strains measured by DIC become relatively large as the magnitude of translation increases.

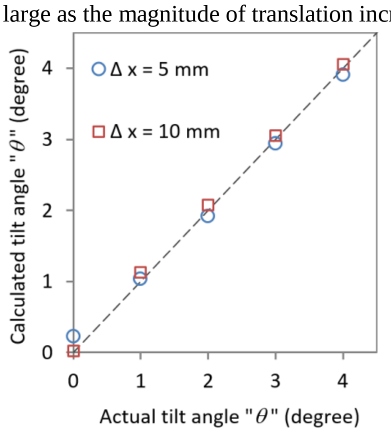

Figure 6. Tilt angles calculated based on normal strain ε_{xx} resulting from translation parallel to the camera plane compared with the actual tilt angles.

4.2. In-plane Translations at an Angle

When performing measurements using any 2D-DIC software, the *x* and *y* directions are typically defined relative to the reference image. By default, the *x* axis is defined in the horizontal direction of the image, and the *y* axis is defined in the vertical direction of the image. It is usually a good experimental practice to align the camera such that the direction of translation of the test specimen is along either the vertical or the horizontal directions of the image (usually the horizontal, since it is larger). As such, it will be possible to translate the specimen along the *x* or *y* directions to verify the camera perpendicularity using the proposed approach before running the actual experiments. However, in some cases it might not be possible to perform a translation along either the *x* or *y* directions, and the translation has to be in some arbitrary (in-plane) direction such that it includes both *x* and *y* components.

The approach presented by Hijazi [37] suggests the use of rigid-body-translations that are in either the *x* or *y* directions. The case where the translation is performed in some arbitrary (in-plane) direction such that it has both *x* and *y* components is considered in this investigation. It should be noted here that such translation in an arbitrary direction is basically a combination of simultaneous Δx and Δy translations. When the camera is not perpendicular to the surface, normal strain error will be induced due to translation in the *x* direction; and when the translation is in the *y* direction, shear strain error will be induced. Thus, both normal and shear strain errors will be induced as a result of a translation having both *x* and *y* components. However, the fact that the strain error equations for *x* and *y* translations are uncoupled (since the *x* translation does not result in shear strain error, and the *y* translation does not result in normal strain error) makes it theoretically possible to use the same existing equations to determine the tilt angle when the translation has both *x* and *y* components. In such case, the tilt angle can be calculated using equation 1 (or equation 2) based on the Δx component of the translation, or it can be calculated using equation 3based on the Δy component of the translation. As mentioned in *section 3.2.2,* the experiments included translations at three different in-plane angles where these angular translations are achieved using simultaneous *x* and *y* translations. It might be worth noting here that the total translation for the 45° case is 4.24 mm (Δx= 3 mm & Δy= 3 mm) while the total translation for the 36.9° and 53.1°cases is 5 mm (Δx= 4 mm & Δy= 3 mm or Δx= 3 mm & Δy= 4 mm). Figure 7 shows the calculated tilt angles for the three cases where the angle for each case is calculated twice, once using equation 1 (based on Δx) and once using equation 3 (based on Δy). For each of these cases, the two equations should theoretically give the same value of the tilt angle. However, as can be seen in the figure, the tilt angles calculated based on the Δx component of the translation are consistently lower than those calculated based on the Δy component. It can also be noted from the figure that the tilt angles calculated based on the Δy component (using ε_{xy}) are fairly close to the actual tilt angle value where the error is about 0.1°, while the error increases to about 0.4° for the tilt angles calculated based on the Δx component (using ε_{xx}). While an error of about 0.4° is not considered to be very high and it might still be acceptable, the fact that it is almost consistent for the three cases might suggest that the simultaneous Δy component of the translation might be somehow slightly affecting the normal strain ε_{xx} error (though the simple theoretical equations being used here do not capture such effect). It might also be likely that this effect is due to the optical aberrations, which generally have more effect on normal stains error than the shear strain error. Regardless of the reason, why such difference between the angles calculated based on normal strain or shear strain is observed; based on the results presented in Figure 7, it is suggested to rely on the shear strain error for calculating the tilt angle for cases of simultaneous *x* and *y* translations.

In real life, scenarios where the direction of translation of the test specimen is not aligned with the image axis, the magnitude of the *x* and *y* components of the translation are not directly known. In such case, the total translation is usually known, and the angle of the translation (with respect to the reference image *x*-axis) can be obtained by comparing the reference and translated images. Based on that, the *x* and *y* components of the translation can be obtained and thus used to calculate the tilt angle.

 © 2021 Jordan Journal of Mechanical and Industrial Engineering. All rights reserved - Volume 15, Number 5 (ISSN 1995-6665)

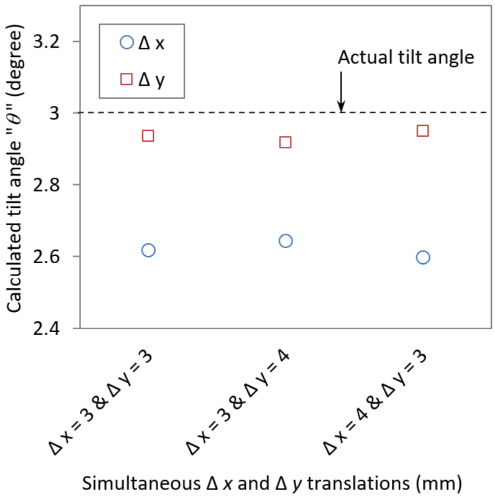

Figure 7. Tilt angles calculated based on the Δx component (using ε_{xx}) and the Δy component (using ε_{xy}) for simultaneous *x* and *y* translation (translation at an angle).

4.3. Two-Axes Tilting (Arbitrarily Oriented Tilt Axis)

The proposed approach assumes that the tilt axis is aligned with the *y* axis (the vertical axis), see Figure 1. In fact, in most cases where 2D-DIC is used, the test specimen (the target surface) will be oriented vertically upwards while the camera is oriented horizontally in order to observe the surface of the specimen perpendicularly. Theoretically, a misalignment might also exist in the vertical or horizontal placement of the specimen or the camera, and thus the target surface can be tilted about the *x* axis. However, from a practical perspective, such misalignment is not of a big concern since it can easily be avoided by using a level-meter (or inclinometer) for checking the horizontal and vertical alignment of the camera and the specimen (nowadays inclinometers are even available as apps for smart phones). Thus, the most concern remains to be about the misalignment (or tilting) about the *y* axis since there is no direct and easy way for detecting such misalignment, and this is where the proposed approach is most useful. Though the proposed approach is mainly focused on the detection of tilt angels about the *y* axis; however, it still can be used for cases where the target surface is tilted about both the *x* and *y* axis. While such case is not very common in experimental mechanics; however, it is worth to be addressed. From a geometric viewpoint, if a surface it rotated about both the *x* and *y* axes, these two rotations can be represented as a single rotation about a new in-plane axis that is neither parallel to *x* nor *y*. While the orientation of this arbitrarily oriented axis, and its tilt angle can be calculated, this is not of concern in our case. Representing any rotation about an arbitrarily oriented in-plane tilt axis through its *x* and *y* rotation components is more useful from the practical point of view, since the *x* and *y* axes represent unique directions that are defined with reference to the camera images. The essence of using the proposed approach for calculating the tilt angles about both the *x* and *y* axes originates from the fact that the strain errors resulting from translation in the *x* and *y* directions are uncoupled (meaning that a translation in the direction perpendicular to the tilt axis causes normal strain error only while a translation in the direction parallel to the tilt axis causes shear strain error only). Therefore, if a translation is performed in the *x* direction while the surface is tilted about both the *x* and *y* axes, this will result in both normal and shear strain errors. The normal strain error ε_{xx} can be used to calculate the tilt angle about the *y* axis (i.e., the axis perpendicular to the translation), while the shear strain error ε_{xy} can be used to calculate the tilt angle about the *x* axis (i.e., the axis parallel to the translation). The tilt angle about the *y* axis is directly calculated using equation 1. However, the tilt angle about the *x* axis is calculated using equation 3 but the Δy in the equation is replaced with Δx (i.e., $\theta_{/\!/} = \tan^{-1}[2\varepsilon_{xy}S/\Delta x]$) since Δx now represents the translation in the direction parallel to the tilt axis. Similarly, if a translation is performed in the *y* direction (instead of the *x* direction), the normal strain error ε_{xx} can be used to calculate the tilt angle about the *x* axis (using equation 1 after replacing Δx with Δy), while the shear strain ε_{xy} error can be used to calculate the tilt angle about the *y* axis (using equation 3). Figure 8 shows the calculated tilt angles about *x* and *y* axes based on *x* direction translation and *y* direction translation. It can be seen from the figure that both the *x* and *y* axes' tilt angles can be calculated with reasonable accuracy (error of less than 0.3°) using a translation in either the *x* or *y* directions. Closer inspection of the calculated tilt angle values shows that for the Δx translation, the *x* axis tilt angle is obtained with higher accuracy than the *y* axis tilt angle. The opposite is also true for the Δy translation where the *y* axis tilt angel has higher accuracy than the *x* axis tilt angle. It should be noted here that the cases where the tilt angles have higher accuracy are those where the shear strain ε_{xy} is used for calculating the tilt angles. This observation is actually consistent with that seen in section 4.2 where this again suggests that the shear strain ε_{xy} is indeed not affected by the translation in the direction perpendicular to the tilt axis. On the other hand, the translation in the direction parallel to the tilt axis apparently has a small effect on the normal strain ε_{xx}, and this causes the slightly higher error for the tilt angles calculated based on the normal strain. While this observation might suggest that the proposed approach is not very accurate when dealing with cases where there is tilting about two axes, this issue can be easily overcome. In order to overcome this issue and to obtain more accurate estimates for both the *x* and *y* axes tilt angles, instead of doing one translation (in the *x* or *y* directions), two translations need to be done once in the *x* direction and once in the *y* direction. As such, the shear strain obtained from the Δx translation can be used for calculating the *x* axis tilt angle accurately, and the shear strain obtained from the Δy translation can be used for calculating the *y* axis tilt angle accurately.

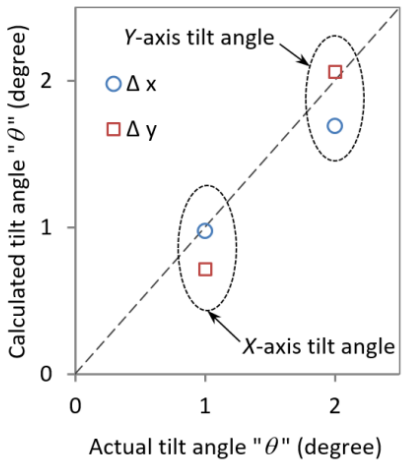

Figure 8. Tilt angles about the *x* and *y* axes calculated using Δx translation and Δy translation.

4.4. Small Translations

The normal and shear strain bias resulting from camera non-perpendicularity are proportional to the magnitude of the rigid-body-translation [37]. In the proposed approach, the strain errors obtained from DIC analysis are used to calculate the tilt angle(s). From theoretical point of view, when the magnitude of strain bias is higher it becomes less affected by the random strain error. Thus, it is expected that a larger magnitude of rigid-body-translation results in more accurate tilt angles. However, it was previously shown that a 5 mm translation (5% of the field-of-view width) results in more accurate tilt angle predictions than larger (10 mm and 15 mm) translations [37]. In this study, the use of rigid-body-translations smaller than 5 mm is investigated to determine if smaller translations can be used for determining the tilt angle with reasonable accuracy. Figure 9shows the tilt angles calculated using small translations in the *x* or *y* directions. Form the figure it can be seen that translations as small as 2 mm (2% of the field-of-view width) can still be used for obtaining the tilt angles with reasonable accuracy. As the magnitude of the translation increases, the accuracy of the calculated tilt angles seems to show a slight improvement. The results shown in the figure suggests that 5 mm translation is probably the most suitable, though translations smaller than 5 mm can be used if necessary.

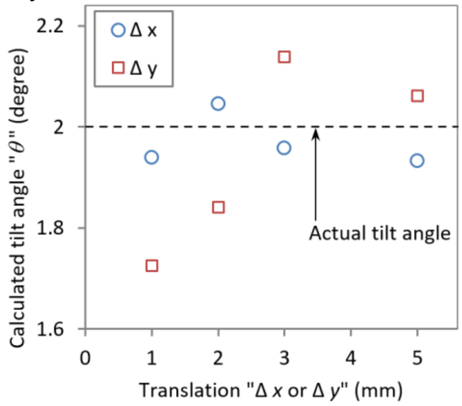

Figure 9. Tilt angles calculated using small Δx and Δy translations.

4.5. Stand-off-distance

The equations being used here to determine the tilt angle(s) are developed based on the pinhole camera model. In a real imaging system, the stand-off-distance (*S*), see Figure 2, represents the distance from the pinhole plane (or the lens mid-thickness if a lens is used) to the target surface. The working distance for a lens is measured from the front end of the lens body to the surface being observed. Multi-element lenses, which are typically used in imaging systems, could be relatively thick sometimes. Determining the exact "optical" mid-thickness plane for a multi-element lens requires the use of some specialized setup. However, the location of the mid-thickness plane for a multi-element lens can be roughly estimated based on physical measurement of the overall thickness of the lens elements. Such approximation of the mid-thickness plane based on physical measurements should be sufficiently accurate for the purpose of estimating the tilt angles using the proposed approach. When determining the tilt angles using any of the equations presented here, the lens working distance has to be augmented by the distance from the lens front end to its mid-thickness. In previous studies [36, 37], 10 mm was added to the lens working distance in order to obtain the stand-off-distance used in the calculations. For the lens used in this investigation, based on the physical measurements, the lens mid-thickness is estimated to be at distance of about53 mm from the front end of the lens body. Therefore, for the experiments performed at 307 mm working distance, the stand-off-distance used in the calculations is 307 + 53 = 360 mm. Similarly, for the other two groups of experiments performed at 197 mm and 417 mm working distance, the stand-off-distance used in the calculations are 250 mm and 470 mm, respectively. Figure 10 shows the calculated tilt angles for three groups of experiments performed at different working distances while the target is tilted at 2°. The figure shows the tilt angles calculated using translations in the *x* direction and the *y* direction where in each case the magnitude of the translation is 5% of the field-of-view width (see *Section 3.2.5*). For each of the calculated tilt angle values shown in the figure, the error bars are also shown. These error bars show the upper and lower limit of the calculated tilt angle values. These upper and lower limit values are obtained by varying the value of the stand-off-distance (*S*) used in the calculations by ±10 mm. From the figure it can be seen that the proposed approach is able to predict the tilt angle with comparable accuracy for the three groups of experiments corresponding to the different stand-off-distance values. The shown error bars for *S* ±10 mm demonstrate that the calculation of the tilt angle is actually sensitive to the value of the stand-off-distance used in the calculation, and it even becomes more sensitive when the stand-off-distance is smaller (e.g., compare the error bars for the 250 mm and 470 mm cases). Therefore, for a lens such as the one that is being used in this investigation, if the working distance is not augmented by the 53 mm, a large error will be introduced in the calculated tilt angles.

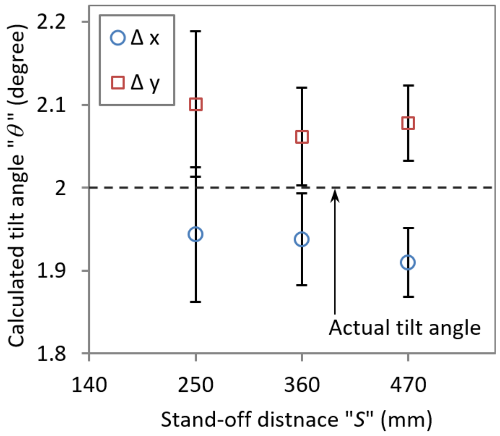

Figure 10. Tilt angles calculated using Δx and Δy translations for experiments performed at different distance from the target (error bars corresponding to S ±10 mm are shown).

5. Concluding remarks

When using the 2D-DIC technique, the camera needs to observe the target surface perpendicularly. If the camera is not perpendicular to the surface, errors will be introduced in both the displacements and strains measured by DIC analysis. Therefore, in experiments where 2D-DIC is to be used, it is imperative to ensure that the camera is properly oriented before starting to make measurements using 2D-DIC. This paper reports on the development of a novel generalized approach for verifying the camera perpendicularity; and if the camera is not perpendicular to the surface, the tilt angle(s) are calculated using this approach. This approach is designed to be performed as an initial setup/calibration procedure before starting to use 2D-DIC in the actual experiments. The tilt angle(s) obtained using this approach may be either used for correcting the camera alignment or, if the alignment cannot be corrected due to some physical limitations, for rectifying the images before they are used for DIC in the actual experiments. The approach is based on performing a simple rigid-body-translation experiment and running DIC analysis to find the strain error(s) caused by camera non-perpendicularity; from that, the tilt angle(s) are calculate using simple analytical equations. Several validations experiments representing different practical scenarios are carried out and the results show that the proposed approach is capable of obtaining the tilt angle(s) with good accuracy. The major conclusions of this study are summarized in the following points:

- When the camera is not perpendicular to the surface, in general, a translation in the direction perpendicular to the tilt axis causes normal strain error (bias), while a translation in the direction parallel to the tilt axis causes shear strain error (bias). The sense of the resulting strain bias depends on the direction of the translation (reversing the direction of translation will reverse the sign of the strain error). As for the magnitude of the resulting strain bias, it mainly depends on three factors: i) the tilt angle, ii) the magnitude of translation, and iii) the distance between the camera and the surface.
- The rigid-body-translation needs to be either parallel to the target plane or parallel to the camera plane. Translation parallel to the target plane can be done by moving the target (this is generally recommended), while the translation parallel to the camera plane can be done by moving the camera itself. Different strain errors are observed in each of the two cases and thus different equations are used for calculating the tilt angle(s) in each case. A translation perpendicular to the tilt axis and parallel to the target plane will cause bias in the two normal stress components (ε_{xx} and ε_{yy}), while it will cause bias only in ε_{xx} (i.e., the normal strain in the direction of translation) when it is parallel to the camera plane.
- A single rigid-body-translation in any in-plane direction is all what is needed to determine the tilt angle(s) using this approach. It is preferred to do the translation along the horizontal or vertical directions of the camera image (i.e., the x or y directions). If necessary, it is also possible to do the translation at an arbitrary in-plane direction (neither parallel nor perpendicular to x and y). In this case, errors will be introduced in both the normal and shear strains, and the angle of translation can be obtained from the images (the angle is used to calculate the x and y components of the translation). Though, theoretically, the tilt angle can be calculated using the normal or shear strain bias, the experiments show that using ε_{xy} gives more accurate results.
- This approach is mainly concerned with cases where the camera/target is tilted about the vertical axis (since alignment with respect to the horizontal axis can easily be verified using simple instruments such as an inclinometer). However, it can also be used for cases where there is tilting about both the x and y axes. In such case, theoretically, a single translation in one direction (x or y) is sufficient for calculating the two tilt angles. But experimental results show that the tilt angles calculated based on the shear strain are more accurate than those calculated based on the normal strain. Thus, it is recommended to do translations in both the x and y direction and use ε_{xy} to calculate the two tilt angles.
- The experiments show that using large magnitude of rigid-body-translation is not necessary for attaining results with good accuracy. A translation equal to 5% of the field-of-view width is found to give good results for all the scenarios that were investigated. If necessary, smaller translations down to 2% of the field-of-view width can be used while maintaining good accuracy for the approach.
- Accurate measurement of the distance between the camera and the target is essential for obtaining good results using this approach. The strain bias resulting from camera non-perpendicularity is inversely related to the stand-off-distance (S). Thus, the smaller the distance between the camera and the target becomes, the more sensitive the results become to small variations in the value of S. The stand-off-distance used in the tilt angle calculation equations is slightly larger than the measured distance between the front end of the lens body and the target surface (i.e., the working distance). For typical small size machine-vision lenses, adding 10 mm to the working distance gives a good approximation for the stand-off-distance. However, for some lenses such as the high-end lens used in this study, larger numbers has to be added to the working distance (based on physical measurements, 53 mm is used for this lens).

Acknowledgements

The author would like to acknowledge the financial support provided by the German research foundation (DFG) for his research visit to Munich Bundeswehr University. The experiments were done in the facilities of the institute of fluid mechanics and aerodynamics at UniBW.

References

[1] Sutton, M. A., Orteu, J. J., & Schreier, H. (2009). Image correlation for shape, motion and deformation measurements: basic concepts, theory and applications. Springer: New York.

[2] Hild, F., & Roux, S. (2006). Digital image correlation: from displacement measurement to identification of elastic properties–a review. Strain, 42(2), 69-80.

[3] Pan, B., Qian, K., Xie, H., & Asundi, A. (2009). Two-dimensional digital image correlation for in-plane displacement and strain measurement: a review. Measurement science and technology, 20(6), 062001.

[4] Orteu, J. J. (2009). 3-D computer vision in experimental mechanics. Optics and lasers in engineering, 47(3-4), 282-291.

[5] Baqersad, J., Poozesh, P., Niezrecki, C., & Avitabile, P. (2017). Photogrammetry and optical methods in structural dynamics–a review. Mechanical Systems and Signal Processing, 86, 17-34.

[6] Hassan, G. M. (2021). Deformation measurement in the presence of discontinuities with digital image correlation: A review. Optics and Lasers in Engineering, 137, 106394.

[7] Niu, Y., Wang, J., Shao, S., Wang, H., Lee, H., & Park, S. B. (2018). A comprehensive solution for electronic packages' reliability assessment with digital image correlation (DIC) method. Microelectronics Reliability, 87, 81-88.

[8] Liljenhjerte, J., Upadhyaya, P., & Kumar, S. (2016). Hyperelastic strain measurements and constitutive parameters identification of 3d printed soft polymers by image processing. Additive Manufacturing, 11, 40-48.

[9] Hijazi, A., Yardi, N., & Madhavan, V. (2004). Determination of forming limit curves using 3D digital image correlation and in-situ observation. Proceedings of the International SAMPE Symposium and Exhibition, Long Beach, CA, 16-20.

[10] Caminero, M. A., Lopez-Pedrosa, M., Pinna, C., & Soutis, C. (2013). Damage monitoring and analysis of composite laminates with an open hole and adhesively bonded repairs using digital image correlation. Composites Part B: Engineering, 53, 76-91.

[11] Feng, D., & Feng, M. Q. (2016). Vision-based multipoint displacement measurement for structural health monitoring. Structural Control and Health Monitoring, 23(5), 876-890.

[12] Cuadra, J., Vanniamparambil, P. A., Hazeli, K., Bartoli, I., & Kontsos, A. (2013). Damage quantification in polymer composites using a hybrid NDT approach. Composites Science and Technology, 83, 11-21.

[13] Eshtayeh, M., Hijazi, A., & Hrairi, M. (2015). Nondestructive evaluation of welded joints using digital image correlation. Journal of Nondestructive Evaluation, 34(4), 1-12.

[14] Pan, B., Tian, L., & Song, X. (2016). Real-time, non-contact and targetless measurement of vertical deflection of bridges using off-axis digital image correlation. Ndt & E International, 79, 73-80.

[15] Libertiaux, V., Pascon, F., & Cescotto, S. (2011). Experimental verification of brain tissue incompressibility using digital image correlation. Journal of the mechanical behavior of biomedical materials, 4(7), 1177-1185.

[16] Soltani, A., Curtze, S., Lahti, J., Järvelä, K., Laurikka, J., Hokka, M., & Kuokkala, V. T. (2018). Digital image correlation study of the deformation and functioning of the human heart during open-heart surgery. In Mechanics of Biological Systems, Materials and other topics in Experimental and Applied Mechanics, Volume 4 (pp. 19-27). Springer, Cham.

[17] Sutton, M. A., Li, N., Joy, D. C., Reynolds, A. P., & Li, X. (2007). Scanning electron microscopy for quantitative small and large deformation measurements part I: SEM imaging at magnifications from 200 to 10,000. Experimental mechanics, 47(6), 775-787.

[18] Rahman, F., Ngaile, G., & Hassan, T. (2021). Optimized stereo digital image correlation setup for miniature round specimen: framework development and implementation. Optics and Lasers in Engineering, 144, 106555.

[19] Kirugulige, M. S., Tippur, H. V., & Denney, T. S. (2007). Measurement of transient deformations using digital image correlation method and high-speed photography: application to dynamic fracture. Applied optics, 46(22), 5083-5096.

[20] Hijazi, A., & Madhavan, V. (2008). A novel ultra-high speed camera for digital image processing applications. Measurement Science and Technology, 19(8), 085503.

[21] Berke, R. B., & Lambros, J. (2014). Ultraviolet digital image correlation (UV-DIC) for high temperature applications. Review of Scientific Instruments, 85(4), 045121.

[22] Bornert, M., Brémand, F., Doumalin, P., Dupré, J. C., Fazzini, M., Grédiac, M., ... & Wattrisse, B. (2009). Assessment of digital image correlation measurement errors: methodology and results. Experimental mechanics, 49(3), 353-370.

[23] Haddadi, H., & Belhabib, S. (2008). Use of rigid-body motion for the investigation and estimation of the measurement errors related to digital image correlation technique. Optics and Lasers in Engineering, 46(2), 185-196.

[24] Hijazi, A., & Kähler, C. J. (2017). Contribution of the imaging system components in the overall error of the two-dimensional digital image correlation technique. Journal of Testing and Evaluation, 45(2), 369-384.

[25] Zhu, H., Liu, X., Chen, L., Ma, Q., & Ma, S. (2018). Influence of imaging configurations on the accuracy of digital image correlation measurement. Measurement Science and Technology, 29(3), 035205.

[26] Hijazi, A., Rawashdeh, N. & Kähler, C. J. (2019). Effect of Camera's Focal Plane Array Fill Factor on Digital Image Correlation Measurement Accuracy. Proceedings of the 5th International Conference on Advances in Mechanical Engineering, Istanbul-Turkey, 537-545.

[27] Chu, T. C., Ranson, W. F., & Sutton, M. A. (1985). Applications of digital-image-correlation techniques to experimental mechanics. Experimental mechanics, 25(3), 232-244.

[28] Sutton, M. A., Yan, J. H., Tiwari, V., Schreier, H. W., & Orteu, J. J. (2008). The effect of out-of-plane motion on 2D and 3D digital image correlation measurements. Optics and Lasers in Engineering, 46(10), 746-757.

[29] Siddiqui, M. Z. (2015). Towards Eliminating the Displacement Bias Due to Out-Of-Plane Motion in 2D Inverse Problems: A Case of General Rigid-Body Motion. Strain, 51(1), 55-70.

[30] Pan, B., Yu, L., & Wu, D. (2013). High-accuracy 2D digital image correlation measurements using low-cost imaging lenses: implementation of a generalized compensation method. Measurement Science and Technology, 25(2), 025001.

[31] Badaloni, M., Lava, P., Rossi, M., Chiappini, G., & Debruyne, D. (2016). Out-of-plane motion evaluation and correction in

© 2021 Jordan Journal of Mechanical and Industrial Engineering. All rights reserved - Volume 15, Number 5 (ISSN 1995-6665)

2D DIC. In Advancement of Optical Methods in Experimental Mechanics, Volume 3 (pp. 181-187). Springer, Cham.
[32] Halding, P. S., Christensen, C. O., & Schmidt, J. W. (2019). Surface rotation correction and strain precision of wide-angle 2D DIC for field use. Journal of Bridge Engineering, 24(4), 04019008.
[33] Meng, L., Jin, G., & Yao, X. (2006). Errors caused by misalignment of the optical camera axis and the object surface in the DSCM. Journal of Tsinghua University, 46(11), 1930.
[34] Lava, P., Coppieters, S., Wang, Y., Van Houtte, P., & Debruyne, D. (2011). Error estimation in measuring strain fields with DIC on planar sheet metal specimens with a non-perpendicular camera alignment. Optics and Lasers in Engineering, 49(1), 57-65.
[35] Wang, L., Chen, Y., Li, H., Kemao, Q., Gu, Y., & Zhai, C. (2020). Out-of-plane motion and non-perpendicular alignment compensation for 2D-DIC based on cross-shaped structured light. Optics and Lasers in Engineering, 134, 106148.
[36] Hijazi, A., Friedl, A., & Kähler, C. J. (2011). Influence of camera’s optical axis non-perpendicularity on measurement accuracy of two-dimensional digital image correlation. Jordan Journal of Mechanical and Industrial Engineering, 5(4), 373-382.
[37] Hijazi, A. (2020). A Novel Approach for the Determination of Surface Tilt Angles in Two-Dimensional Digital Image Correlation Experiments. Experimental Mechanics, 60(3), 267-282.
[38] MatchID-2D manual: <www.MatchID.org>